GEOCHEMISTRY

An Early Cretaceous subduction-modified mantle underneath the ultraslow spreading Gakkel Ridge, Arctic Ocean

Marianne Richter[1,2]*, Oliver Nebel[1,2], Roland Maas[3], Ben Mather[4], Yona Nebel-Jacobsen[1,2], Fabio A. Capitanio[2], Henry J. B. Dick[5], Peter A. Cawood[1,2]

Earth's upper mantle, as sampled by mid-ocean ridge basalts (MORBs) at oceanic spreading centers, has developed chemical and isotopic heterogeneity over billions of years through focused melt extraction and re-enrichment by recycled crustal components. Chemical and isotopic heterogeneity of MORB is dwarfed by the large compositional spectrum of lavas at convergent margins, identifying subduction zones as the major site for crustal recycling into and modification of the mantle. The fate of subduction-modified mantle and if this heterogeneity transmits into MORB chemistry remains elusive. Here, we investigate the origin of upper mantle chemical heterogeneity underneath the Western Gakkel Ridge region in the Arctic Ocean through MORB geochemistry and tectonic plate reconstruction. We find that seafloor lavas from the Western Gakkel Ridge region mirror geochemical signatures of an Early Cretaceous, paleo-subduction zone, and conclude that the upper mantle can preserve a long-lived, stationary geochemical memory of past geodynamic processes.

INTRODUCTION

Compositional variations in Earth's upper mantle, as sampled along oceanic spreading centers, range from over thousands of kilometers (*1*, *2*) to the subkilometer scale (*3*, *4*). While many questions about the physical extent, age, and chemical-mineralogical composition of mantle heterogeneity remain outstanding (*5*), it is clear that these form by a combination of earlier melting events and mantle re-enrichment associated with recycling of crustal components (*6*). Well-known examples of compositionally diverse upper mantle include supra-subduction zone mantle, lithospheric mantle under cratons, and possibly plume-infused mantle (*7*). Some mid-ocean ridge basalts (MORBs) carry radiogenic isotopic signatures interpreted as either subduction zone–modified mantle (*8*–*11*), relics of ancient mantle plume activity (*12*, *13*), or remnants of cratonic lithospheric mantle (*2*, *14*). It remains, however, unclear to what extent the compositionally diverse upper mantle contributes to the chemical diversity in basalts, in particular at divergent plate boundaries.

To examine this, the ultraslow spreading Gakkel Ridge in the Arctic Ocean was chosen as a natural laboratory due to (i) reported extreme mantle chemical heterogeneity (*15*, *16*), (ii) along-ridge variations in axial depth (*17*), and (iii) magma production rate (*13*) and crustal thickness (*18*). All these traits are potential expressions of mantle source heterogeneity (*19*) and are potentially linked to a complex tectonic evolution in the circum-Arctic region (*20*, *21*).

At present, the circum-Arctic region consists of two major basins, the Eurasia basin and the Amerasia basin, orthogonal to each other and divided by the Lomonosov Ridge (Fig. 1) (*21*, *22*). During the Jurassic and the Cretaceous, the circumpolar region was affected by various subduction events, opening and closing of ocean basins, accretion of terranes, and large igneous provinces (*20*, *21*, *23*). Dredged MORBs from the Western Gakkel Ridge region studied here have previously been linked to stranded subcontinental lithospheric mantle (SCLM) (*14*), highlighting the complex nature of the upper mantle in this region.

The nature of the mantle source of the MORBs at the Gakkel Ridge is assessed here by combining geochemical observation and placing them in context with paleogeographic reconstruction of the circumpolar region. We present geochemical and paleogeographical evidence that the basalt from the Western Gakkel Ridge region resembles an arc to back-arc transition, linked to the Early Cretaceous South Anuyi subduction event that occurred in the study area between 145 and 125 million years (Ma).

RESULTS

Distinct geochemical signature of the Western Gakkel Ridge region

The Western Gakkel Ridge region consists of two ridge segments, the Western Volcanic Zone (WVZ) and the Sparsely Magmatic Zone (SMZ) (Fig. 1). Both ridge segments are geochemically distinct, showing differences in their trace element patterns (Fig. 2A). Basalts from the WVZ follow a rather back-arc basin basalt (BABB) trend than N-MORB (normal MORB) trend, whereas basalts from the SMZ are alike E-MORBs (enriched MORBs; Fig. 2A). The most notable feature in basalts from both ridge segments is the enrichment in fluid-mobile elements, Ba and Sr, and the depletion in Th (incompatible element) compared to E-MORB or N-MORB (Fig. 2A and fig. S1). These elemental enrichment and depletion patterns are generally unusual for MORBs and cannot be explained by a single-stage melting event. It rather suggests a complex history of melt extraction and re-enrichment in the upper mantle beneath the Western Gakkel Ridge region (*15*, *16*, *24*).

New trace element and isotopic data for dredged lavas from both ridge segments, analyzed in this study, support the inference of an

[1]Isotopia Laboratory, School of Earth, Atmosphere and Environment, Monash University, Clayton, Victoria 3800, Australia. [2]School of Earth, Atmosphere and Environment, Monash University, Clayton, Victoria 3800, Australia. [3]School of Earth Sciences, University of Melbourne, Parkville, Victoria 3010, Australia. [4]School of Geosciences, The University of Sydney, Sydney, New South Wales 2006, Australia. [5]Department of Geology and Geophysics, Woods Hole Oceanographic Institution, Woods Hole, MA 02543-1539, USA.
*Corresponding author. Email: marianne.richter@monash.edu

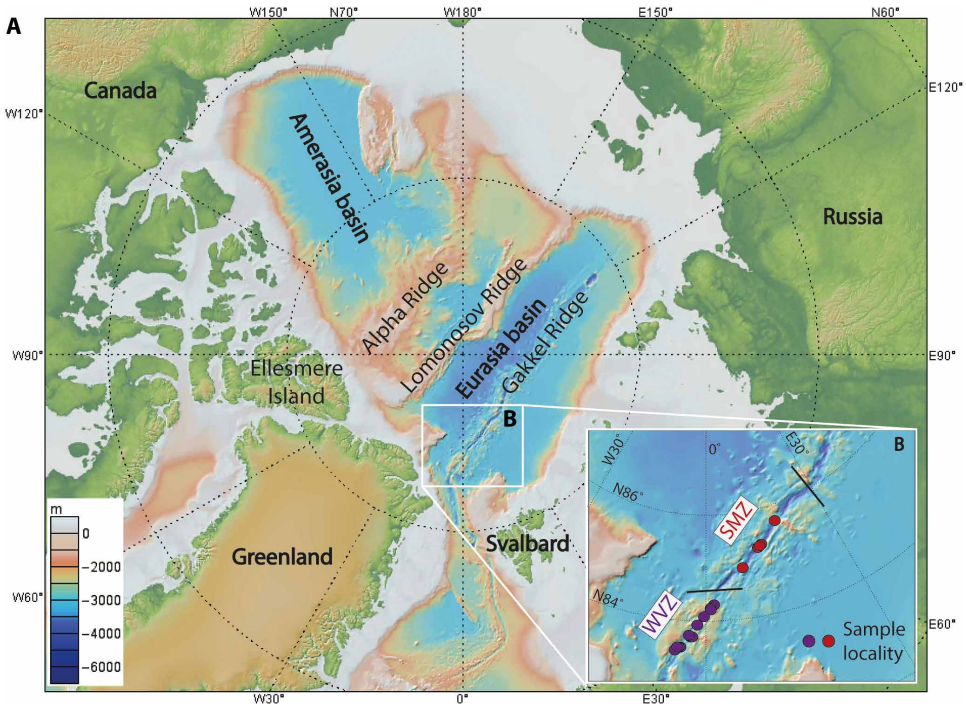

Fig. 1. Geographical overview and sample locality. (**A**) The ultraslow-spreading Gakkel Ridge extends for ca. 1800 km from the northwest coast of Greenland to the northern coast of Siberia and is located in the Eurasia basin. The Western Gakkel Ridge region is highlighted as a white square, and a zoomed-in view is provided in (**B**). The Western Gakkel Ridge region is divided, here, in the WVZ and the SMZ. The purple and red dots represent the sample locality of the basalts from the WVZ and SMZ, respectively. The exact location of each sample is provided in table S1. The maps were made using GeoMapApp (www.geomapapp.org).

extremely chemical heterogeneous upper mantle similar to those found in regional abyssal peridotites (*15*, *16*) and are coherent with previous trace element and isotope studies from this region (*14*, *17*, *25*, *26*).

Despite the enrichment and depletion in the SMZ and the WVZ basalts, both ridge segments are further characterized by elevated $^{87}Sr/^{86}Sr$ isotope signature for a given $^{208}Pb/^{204}Pb$ compared to Atlantic or Pacific MORBs (Fig. 3A) (*14*). These elevated isotopic anomalies, as found in the Gakkel Ridge basalts, are indicative of a crustal component (*8*, *14*) in the MORB source.

These isotopic anomalies in the Western Gakkel Ridge lavas were previously ascribed to an SCLM origin (*14*, *27*). In this model, SCLM underlying greater Greenland became detached, after the continental breakup of Greenland and Spitsbergen at around 50 Ma, and integrated in the present-day MORB source. Various isotopic studies, however, argue against a possible detachment of SCLM in the greater Western Gakkel Ridge region (*28*–*31*). Noble gas systematics in abyssal peridotites from the Lena Trough, adjacent to the Western Gakkel Ridge, indicate that this area underwent a degassing event, which cannot be solely explained by a "long-lived and deep-seated mantle enrichment" (*30*). This controversy leaves the origin of the chemical and isotopic anomaly in the mantle underpinning the Gakkel Ridge ambiguous. Negative buoyancy is the most common driving force for lower continental lithospheric delamination, and in the case of the Gakkel Ridge region, because of the subtle nature of the geochemical variability, only a small volume of lower lithospheric sections can plausibly have delaminated (*32*).

The sum of previously published Gakkel Ridge data and new data obtained in this study, combined with the now available global ocean floor data (*14*, *26*), allows a detailed assessment of the nature of the mantle source and the distinct geochemical and isotope signature found in the Western Gakkel Ridge basalts. Here, we propose an alternative explanation with reference to a paleo-subduction zone, which, given the sum of geodynamic, paleo-reconstruction, and geochemical constraints, appears a more feasible scenario to explain the distinct trace elemental and isotopic signature found in the Western Gakkel Ridge region.

Elemental depletion and enrichment patterns of the Western Gakkel Ridge basalts

To assess potential prior melt extraction and re-enrichment of the Gakkel Ridge MORB source, we compare large ion lithophile element (LILE; Rb, Ba, and Sr) and high-field strength element (HFSE; Zr, Nb, and Hf) concentrations with global MORB data and convergent margin lavas. A first indication of a preconditioned mantle source in the Western Gakkel Ridge region is Zr/Nb, which is an indicator for prior melt extraction (*33*). Niobium and Zr have a similar, yet not identical, incompatibility during partial mantle melting, with Nb being slightly more incompatible than Zr. Melt extraction caused by partial (fluxed) melting may produce lower Zr/Nb in melts, which increases Zr/Nb in the mantle residue. Subsequent melt extraction from such a residual mantle sources will produce second-stage melts with a memory of this prior depletion, generally through higher Zr/Nb, enhanced through Nb depletion. Basalts from the WVZ show systematically higher Zr/Nb than lavas from the SMZ, broadly bracketing average MORB composition and suggesting that the WVZ basalts record a memory of a prior melting event (fig. S2B).

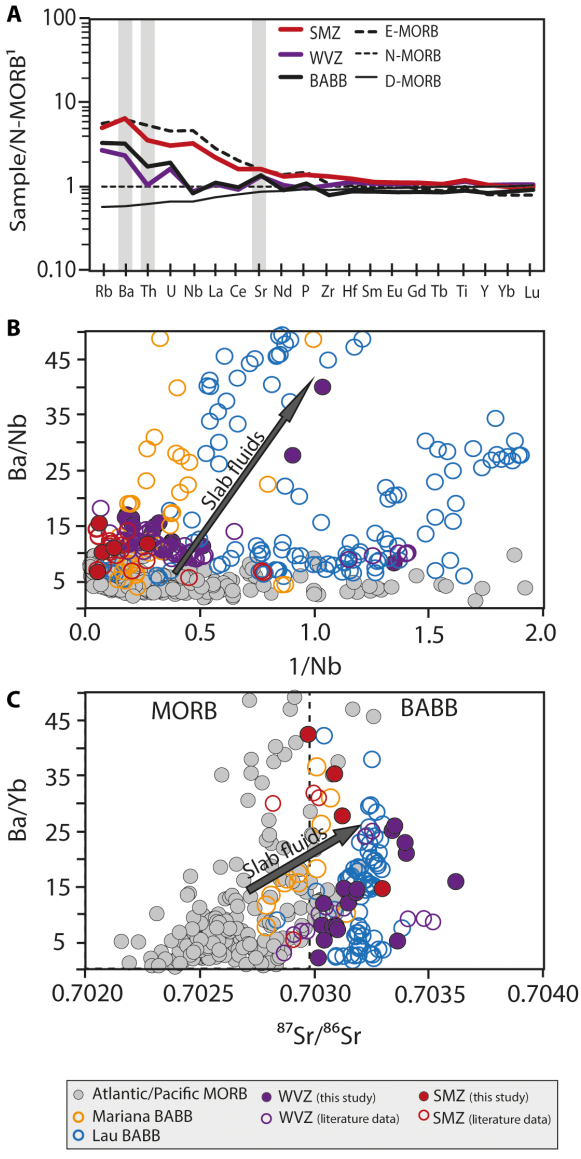

Fig. 2. Trace element pattern and chemical proxies of past subduction influence. (**A**) The average trace element composition of the basalts from the Western Gakkel Ridge region is plotted relative to N-MORB showing an enrichment in fluid mobile elements (Ba and Sr), similar to BABBs. The similarity to BABB is further supported by (**B**) and (**C**). A detailed trace element plot can be found in fig. S1. Data for N-, D-, and E-MORB and BABB are plotted for comparison and taken from Gale *et al.* (*63*) (B), and (C) basalts from the Western Gakkel Ridge region show a pronounced enrichment in Ba and $^{87}Sr/^{86}Sr$ (up to 0.7037) compared to MORBs from the Atlantic and Pacific, similar to active island-arc and back-arc basins, such as the Lau and Mariana back-arc basin. High $^{87}Sr/^{86}Sr$, Ba/Yb, and Ba/Nb ratios are explained by partial melting of a fluid-enriched mantle source. SMZ basalts tend to have higher Ba/Yb and lower Ba/Nb than WVZ basalts, implying a higher degree of source enrichment. Atlantic/Pacific MORB and Mariana BABB and Lau BABB data, plotted here for comparison, are compiled from Gale *et al.* (*63*). MORB data from the pacific include all values from ridge segments ranging between 15°N and 33°S and from the Atlantic ranging between 30°N and 30°S. Literature data from WVZ and SMZ are compiled from Gale *et al.* (*63*) and Goldstein *et al.* (*14*).

Despite the differences in Zr/Nb of the WVZ and SMZ lavas, interpreted here as a memory of variable degrees of melt depletion, a second indication of a preconditioned mantle source beneath the Western Gakkel Ridge region is the enrichment of Ba in the WVZ and SMZ lavas (Figs. 2 and 3B). Barium is a fluid-mobile element and is commonly associated with island-arc and back-arc basin lavas (*34*, *35*), but at present, the Gakkel Ridge is an active spreading ridge. Thus, the Ba enrichment observed in the Western Gakkel Ridge basalt must record past tectonic processes (possibly fluid enrichments) that chemically modified the upper mantle in this area. To test whether the upper mantle beneath the Western Gakkel Ridge region was affected by subduction-induced fluid, Ba/Nb (Fig. 2B), Ba/Yb (Fig. 2C and fig. S2C), and Ba/Th (Figs. 3B and 4), which are all potential tracers for subduction input (*33*), are used here to characterize the MORB source. To assess the role of fluids, Western Gakkel Ridge basalts are compared with BABBs from the Western Pacific and basalts from the Mid-Atlantic Ridge and the Eastern Pacific Rise, the latter being a type locality of MORB showing no known influence of enriched mantle components. The comparison reveals that some basalts from the Western Gakkel Ridge region fall within the MORB field, whereas others plot slightly outside of it and co-align with BABBs from the Western Pacific region (Figs. 2 to 4).

DISCUSSION

Memory of a "ghost-arc" signature in the circum-Arctic mantle

Indices of prior melt depletion in incompatible elements and re-enrichment in fluid mobile elements are unusual for mid-ocean ridge lavas. Here, we argue that these geochemical signatures are a memory of a past subduction zone underpinning the Western Gakkel Ridge region and, in the following, outline a feasible scenario in the paleo-Arctic region. A residual geochemical subduction signature, as is the case for the source of BABB, is expected in mantle with a prior subduction history. Geochemical proxies indicative for past subduction activity (e.g., Zr/Nb and Ba/Yb) in MORBs, here defined as "ghost-arc" signatures, are expected to be subtler in melts derived from a mantle that retains only a memory of a past subduction activity, similarly to the differences between back-arc and arc lavas. Such ghost-arc signatures, typically found in BABB, are distinct from ordinary MORB sources, such as those of the East Pacific Rise, but appear similar to those of the Western Gakkel Ridge. In an active arc environment, dehydration melting of the subducting slab brings the full slab component from slab to the overlying arc, whereby in a back arc, only geochemical pollutants of this process remain in the mantle and can be traced in melts derived thereof, resulting in "soft arc signatures" in BABBs. Solely volumetrically small components of the subduction zone enrichments remain in the mantle wedge in the upper mantle. These remnants are the components of interest here and are argued to be traced by the Western Gakkel Ridge MORBs. Indications of a past subduction relate to mantle (re-)enrichment in fluid-mobile elements (Sr and Ba), as well as variable Zr/Nb in both WVZ and SMZ lavas, which is consequent to prior melting of a hot mantle wedge to variable degrees (*36*).

In addition to this geochemical memory of past subduction activity, paleogeographic reconstructions of the high Arctic region further support the plausibility that the Gakkel Ridge MORBs mirror chemical signature of a BABB and/or a mantle wedge from a paleo-subduction zone. Previous paleogeographic reconstructions and seismic tomography studies from the greater Arctic region show the presence of a past subduction zone, related to the closure of the South Anuyi Ocean (SAO), in the Early Cretaceous (145 to 125 Ma) (*20*, *21*, *23*, *37*). A study by Shephard *et al.* (*23*) shows that geochemical

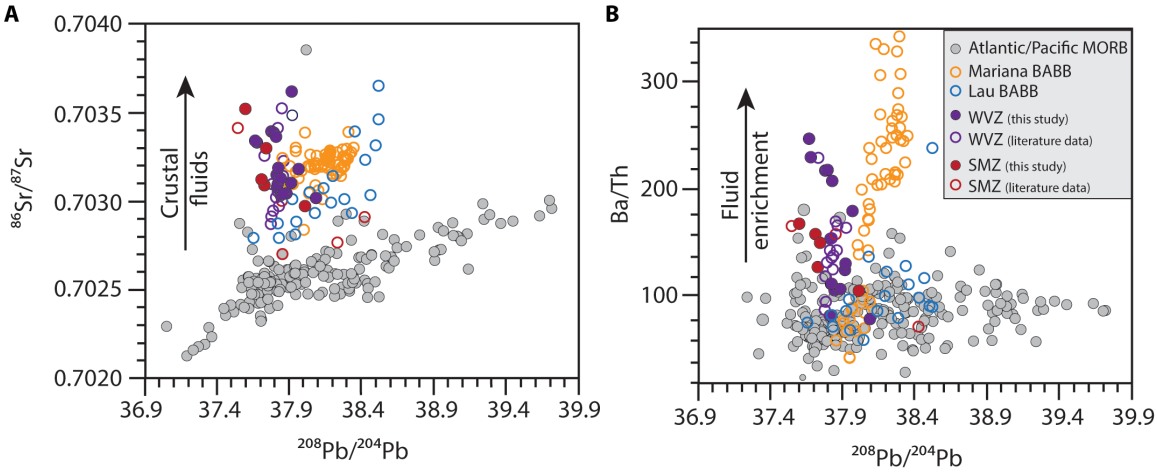

Fig. 3. Sr-Ba-Th systematics versus $^{208}Pb/^{204}Pb$ of the Western Gakkel Ridge basalts. (**A**) Distinct Sr composition of the Western Gakkel Ridge basalts compared to Atlantic/Pacific MORB. (**B**) Ba-Th versus $^{208}Pb/^{204}Pb$ shows similarities to Sr-Pb systematics. Western Gakkel Ridge basalts plot in the same range as BABB from the Lau basin and Marianas. Atlantic MORB data range from 30°N to 30°S, whereas the Pacific MORB data comprise solely data from the Eastern Pacific Rise ranging from 12°N to 30°S. Mariana and Lau BABB data were compiled from Gale *et al.* (*63*). The literature data for the WVZ and the SMZ are compiled from Gale *et al.* (*63*) and Goldstein *et al.* (*14*). Sr and Pb data for this study are provided in table S2.

signatures of tholeiitic and alkaline samples from the Sverdrup basin (Ellesmere region) in northeastern Canada are consistent with an SAO subduction zone, which is further supported by seismic tomography and gravity models from the Ellesmere region and central Greenland (fig. S3). Both seismic tomography and gravity models show an oceanic slab component, linked to the SAO subduction zone, residing beneath central Greenland at a depth of 1300 to 1500 km (*23*, *37*). The extent to which the SAO subduction zone affected other parts in the circumpolar region remains unclear.

It is, however, clear that the present-day Western Gakkel Ridge regions falls into the influence of the SAO. Paleo-reconstructions from the greater Arctic region, conducted here, suggest the presence of an SSW-facing subduction zone that transgressed across the Western Gakkel Ridge region between 145 and 130 Ma (Fig. 5 and fig. S3). We propose that during this time, the regional upper mantle became chemically modified, evidenced by a calculated high slab flux (fig. S4B), with the SMZ as rear-arc region and the WVZ as back-arc region (Fig. 5). The preserved subduction zone setting is ascribed here to the closure of the SAO ~130 Ma ago (Fig. 5) (*20*). Calculated subduction volume and slab flux models (fig. S4), as well as paleogeographic reconstruction, show the potential regional extent of the SAO subduction zone and suggest that the Western Gakkel Ridge region forms the westernmost boundary of the SAO subduction zone (fig. S3).

Origin of modified mantle sections and thorogenic Pb

The geochemical signatures in the Western Gakkel Ridge region require a form of modified mantle source, previously argued to be stranded lithospheric mantle (*14*) but argued here to be, most likely, consistent with subduction-modified mantle. For the latter scenario, which aligns with the paleo-reconstruction, we endeavor to further offer a realistic scenario for mantle modification. The physical form of inherited subduction-type Ba-Th versus Sr isotope systematics in the Gakkel Ridge mantle is examined within a slab mélange model (*38*–*40*). In this model, mélanges consisting of hydrous thin veneer of subducted sediments and depleted mantle peridotites ascend diapirically (*40*) from the subducting slab into the mantle wedge due to buoyancy differences (Fig. 5). In the mantle wedge, the mélange diapirs undergo dehydration melting forming the source for arc magmas, leaving a depleted residue (recorded in elevated Zr/Nb). The presence of mélange diapir remnants, marked by fossil melting residues of a former mélange plume (Fig. 5), provides a more plausible physical model for chemical mantle modification in the mantle wedge than a purely fluid-based metasomatic model, based on recent evidence for physical residues of sediment melting in the center of a former mantle wedge (*40*). In the case of the Gakkel Ridge, we propose that, after subduction ceased, the mélange remnants remain neutrally buoyant and stationary in the area due to re-equilibrating (mostly thermal) density differences with the ambient mantle. With the opening of the Gakkel Ridge, mélange residues became integrated into the upwelling mantle (Fig. 5) and are sampled by the present-day Gakkel MORBs. Notably, this scenario poses the equivalent to stationary delaminated, melt-depleted, and partly re-enriched lithospheric sections. Geochemical proxies look similar in either scenario, because lithospheric enrichment is also often induced through subduction processes, except for enrichments in HFSE (in SCLM) as opposed to their depletion [subduction zone (SZ)].

Critical to the mélange model is the redelivery of Th into the mantle wedge, along with fluid-borne Ba-Sr. Gakkel Ridge lavas have relatively high thorogenic Pb isotope ratios (high $^{208}Pb/^{204}Pb$) compared to global MORB (fig. S5), requiring a history of elevated Th/Pb and Th/U in their mantle source. Elevated Th/Yb in MORBs (Fig. 6A) is diagnostic for, and sensitive to, the influence of a subduction component in their mantle source (*35*, *39*). The Th-Nb/Yb compositions of the Gakkel Ridge basalts (Fig. 6A) lie at the upper boundary of the MORB field and, combined with high $^{208}Pb/^{206}Pb$, imply high time-integrated Th/U, with ^{232}Th being the parent nuclide of ^{208}Pb and ^{238}U being the parent nuclide of ^{206}Pb, in its mantle source (Fig. 6B). If high time-integrated Th/U existed in the mantle source beneath the present-day Western Gakkel area since subduction ceased at ca. ~130 Ma, as proposed by our model, elevated $^{208}Pb/^{206}Pb$ may be explained as the result of local thorogenic ingrowth in high Th/U zones inherited from fossil mélange rocks in the underlying mantle.

Mass balance considerations were used to infer that up to 70% of the original Th may be retained when subducted sediments undergo

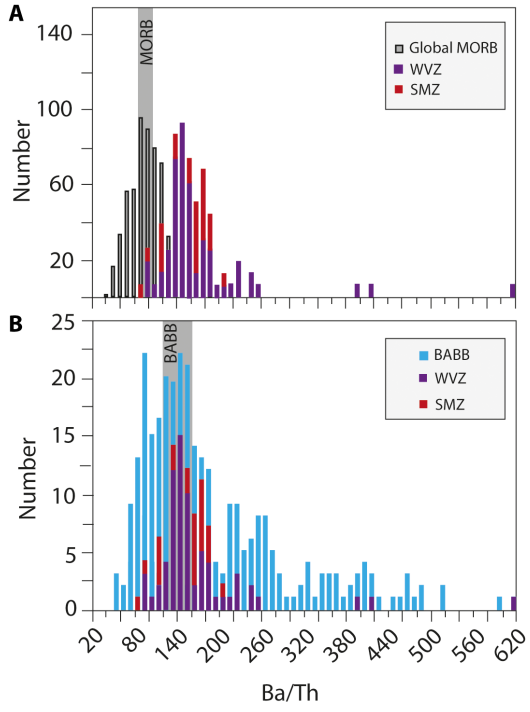

Fig. 4. Ba/Th in MORB from the Western Gakkel Ridge region. Distribution of Ba/Th of the Western Gakkel Ridge MORBs (SMZ and WVZ) compared with global MORB data (**A**) and BABB (**B**). Ba/Th in SMZ basalts is higher than that in WVZ basalts, and Ba/Th in both ridge segments tend to be high compared to the global MORB distribution. Western Gakkel Ridge basalts, however, show a considerable overlap with Ba/Th in basalts erupted in active back-arc basins. MORB data are from Jenner and O'Neill (*64*), and BABB data are from Gale *et al.* (*63*) including Lau and Mariana BABB data. The gray bar represents the average Ba/Th concentration of MORB and BABB. Atlantic/Pacific MORB and Mariana BABB and Lau BABB data, plotted here for comparison, are compiled from Gale *et al.* (*63*). MORB data from the Pacific include all values from ridge segments ranging between 15°N and 33°S and from the Atlantic ranging between 30°N and 30°S. Literature data from the WVZ and the SMZ are compiled from Gale *et al.* (*63*) and Goldstein *et al.* (*14*).

dehydration or partial melting (*41*). Assuming that these high Th/U residual mélange complexes remain within the upper mantle once subduction ceases, ingrown high $^{208}Pb/^{206}Pb$ would be expected to be mobilized in younger melting episodes, such as for the modern Gakkel Ridge MORB magmatism. A near-identical component was traced behind the Mariana arc (*35*), adding further weight to this scenario.

Simple radiogenic Pb ingrowth modeling at a time scale $t = 130$ Ma (inferred from the last subduction activity in the Gakkel Ridge area) indicates that a $^{232}Th/^{238}U$ (κ) ~ 5.6 is required to generate the observed ^{208}Pb isotope ingrowth (high $\Delta^{208}Pb^*/^{206}Pb^*$; Fig. 6B) observed in the Western Gakkel Ridge lavas compared to Atlantic and Pacific MORB. This calculation is based on the assumption that the starting composition of the Pb isotope composition is identical to the Northern Hemisphere Reference Line (NHRL) (fig. S5) and that the basalts originate from a melt-depleted mantle with a $^{238}U/^{204}Pb$ (μ_{DM}) = 6.33 (*42*), whereby U is stripped off during primary melt extraction in the arc. The $^{238}U/^{204}Pb$, in combination with a $^{232}Th/^{238}U$ (κ), suggests a Th enrichment in residual assemblages, leading to a $^{232}Th/^{204}Pb$ (ω) = 35.1 in the sub–Gakkel Ridge mantle.

In addition, remarkably homogeneous Pb isotope compositions along the length of the Western Gakkel Ridge indicate a homogeneous distribution of Th/U in the mantle along the entire length of the magmatically active ridge. Fossil diapir regions in the sub-ridge mantle, enriched in Th, occur most likely only locally (e.g., Th-rich accessory minerals formed during Early Cretaceous mélange diapir melting), and such domains are presumably higher in Th/U than required by the time-integrated average calculated κ for Gakkel Ridge lavas. A feasible solution to this conundrum is that partial melts are homogenized before eruption, possibly by diffusion in a melt network or in sub-oceanic magma ponds (*43*). Only small amounts of an enriched ^{208}Pb isotope component are sufficient to shift melts off the NHRL (toward a higher $^{208}Pb/^{204}Pb$ for a given $^{206}Pb/^{204}Pb$), whereas other signatures, such as element ratios or Sr isotopes, are much less susceptible to change.

Comparison to the SCLM model and Arctic perspective

Elevated $^{208}Pb/^{204}Pb$ and $^{87}Sr/^{86}Sr$ isotope signatures in the Western Gakkel Ridge region were previously linked to the incorporation of delaminated SCLM due to the propagation of the North Atlantic mantle into the Arctic asthenosphere at ~56 Ma (*14*, *27*). The integration of SCLM was further supported by elevated Rb/Sr, Rb/La, and Th/La in the Western Gakkel Ridge basalts (*14*). These elemental enrichment patterns were previously associated with alkaline basalts from Spitsbergen and attributed to melting in the presence of amphibole and phlogopite in the MORB mantle (*14*, *27*). Both are hydrous mineral phases that, when incorporated into the melting column, can lead to elevated alkali (e.g., Rb) and trace elemental signatures (Th). While the observations are coherent with an SCLM origin, both phases are not exclusively stored in SCLM. Amphibole and phlogopite can be present in subduction-related environments (*44*), which is favored in our model. A similar origin can be ascribed to the unusually elevated Rb and Ba concentrations in the Western Gakkel Ridge basalts by the presence of phengite in the MORB source. Phengite is a potassium-rich white mica incorporating LILE (Rb, Ba, Cs, and K) and is stable up to 150-km depth in subducting environments (*39*, *44*–*46*). In a subduction-driven setting, two possible scenarios can occur in the Western Gakkel Ridge region. First, phengite dehydration occurred during active subduction and ultimately enriched the mélange diapirs with metasomatic fluids, or second, the mélange diapirs contain residual phengite that can contribute to elevated Ba and Rb ratios in a subsequent melting event (*39*), as potentially occurred in the Western Gakkel Ridge region. Notable is that all observed geochemical features can also be produced by small-volume delamination of continental lithosphere, which was infused by metasomatism during past subduction events.

From a geochemical perspective, either scenario that of an SCLM source or a past subduction zone seems plausible. However, with the supporting evidence from seismic data (*47*, *48*), paleo-reconstructions of a past subduction zone (*20*, *21*, *23*, *49*, *50*), the arc/back-arc progression from the SMZ to the WVZ, and geochemical proxies commonly associated with subduction-modified mantle, a past subduction zone appears a superior scenario. We therefore argue that the Western Gakkel Ridge basalts sample an area of the upper mantle that is chemically modified by the SAO subduction zone during the Early Cretaceous.

We cannot draw any conclusion to which extent the SAO subduction zone affected other parts of the greater Arctic region due to a lack of suitable samples. This also accounts for whether, and if so to which extent, the HALIP, which was active after the SAO subduction zone ceased, affected the chemistry of the Arctic MORB. A

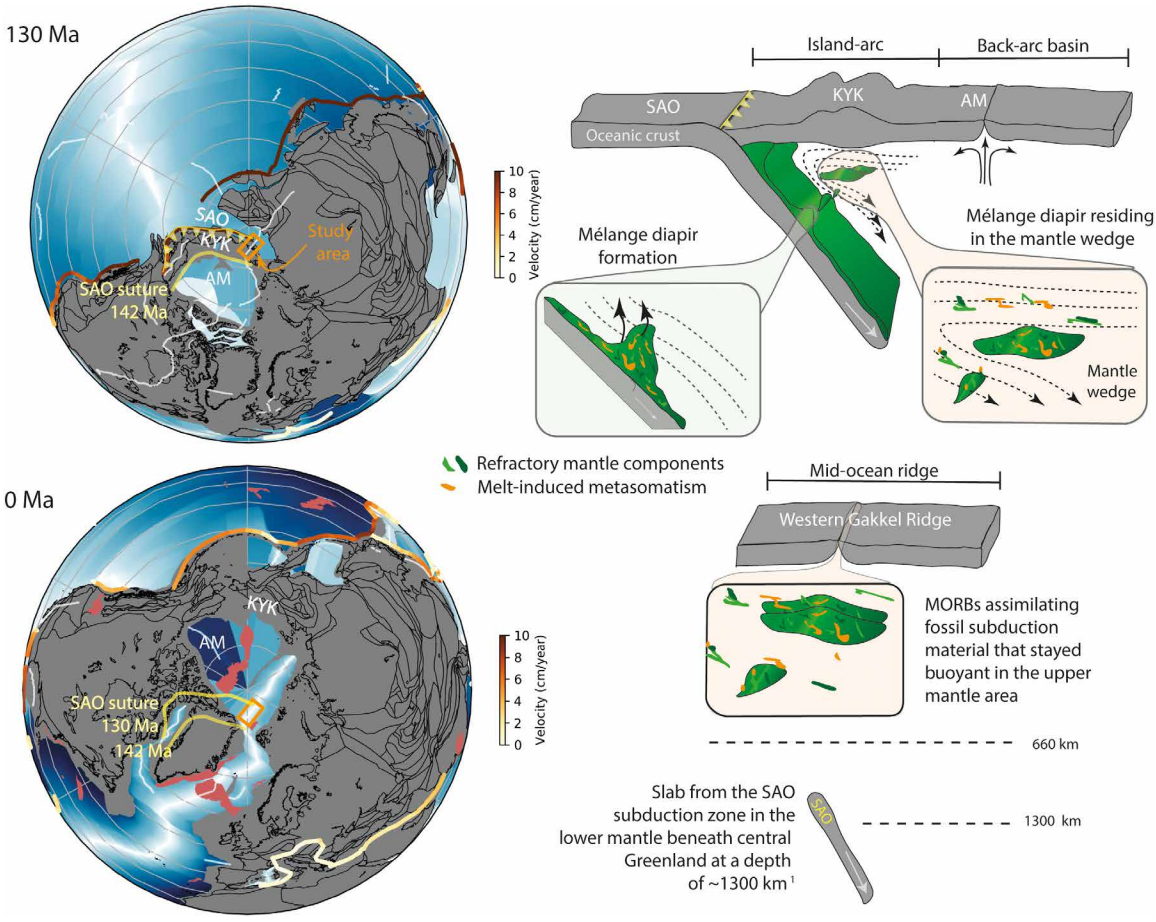

Fig. 5. Paleogeography of the circum-Arctic region. Paleogeographic reconstructions show the Arctic region during the closure of the SAO at 130 Ma (**top**) and the present day (**bottom**). Top: During the closure and subduction of the SAO, mélange diapirs ascend into the mantle wedge, forming the Koyukuk-Nutseyn (KYK) volcanic arc at 145 to 130 Ma, which also led to the opening of the Amerasia basin (AM), which operated until 120 Ma as back-arc basin (*50*). The bottom panel at present-day shows the location of the SAO suture zone at 142 Ma (onset of subduction) and at 130 Ma (closure of SAO subduction). The red areas highlight the areas of the large igneous provinces. The orange rectangle in the paleo-reconstruction models highlights the sample locality, and on the right of the present day is our suggested model. Mélange diapirs, resultant from the SAO subduction, stay buoyant in the upper mantle and became integrated into the source of the Western Gakkel Ridge region. The slab of the SAO subduction resides at a depth of ~1300 km in the lower mantle (*23*). All paleogeographic reconstructions can be reproduced using pyGPlates (www.gplates.org).

detailed geochemical assessment is required to understand the complex tectonic evolution and upper mantle heterogeneity in the greater Arctic region.

Global perspective for subduction inheritance in the upper MORB mantle

Apparent similarities between the Gakkel Ridge and the Australian-Antarctic Discordance (AAD), a prominent seafloor depression at the Southeast Indian Ridge between Australia and Antarctica, indicate that the proposed subduction feature in sub-ridge mantle is not an oddity confined to the Arctic Ocean. The ridge depression along the AAD is coupled with lower magmatic activity and upper mantle depletion (*19*, *51*), and Pb isotope compositions along the depressed section of the ridge differ from those outside the AAD. These features were tentatively linked to a stagnating slab residing in the upper mantle left behind from long-lived subduction along the Eastern Gondwana margin 570 to 130 Ma (*51*–*54*), possibly providing another example of a sub-ridge fossil subduction system. Furthermore, the Gakkel Ridge lavas not only share geochemical similarities in LILE, HFSE, and Sr isotopes with those of arc/back-arc lavas of Western Pacific subduction zones, e.g., the Mariana and Lau back-arc basins, but also resemble their $^{208}Pb/^{206}Pb$ (Th/U) systematics of Indian-type mantle (Fig. 6B), which, in turn, have compositions reminiscent of DUPAL-type mantle (*53*).

Conclusion

The preservation of an MORB suite with rear-arc (SMZ) to back-arc (WVZ) geochemical-isotopic signatures and its link to the SAO paleo-subduction zone provide insights into regional tectonic processes and indicate a lower boundary to the survival time of subduction-modified mantle, possibly in the form of mélange diapirs/wedge plumes, after subduction cessation. The presence of these sections that remain stationary in the upper Earth's mantle further implies that subduction leaves a chemical footprint, which, with time, can add to the chemical heterogeneity in global MORB without a deep mantle cycling. As a consequence, geochemical signatures of MORBs in combination with paleogeographic reconstructions not only contribute to a regional tectonic history but also provide a glimpse into

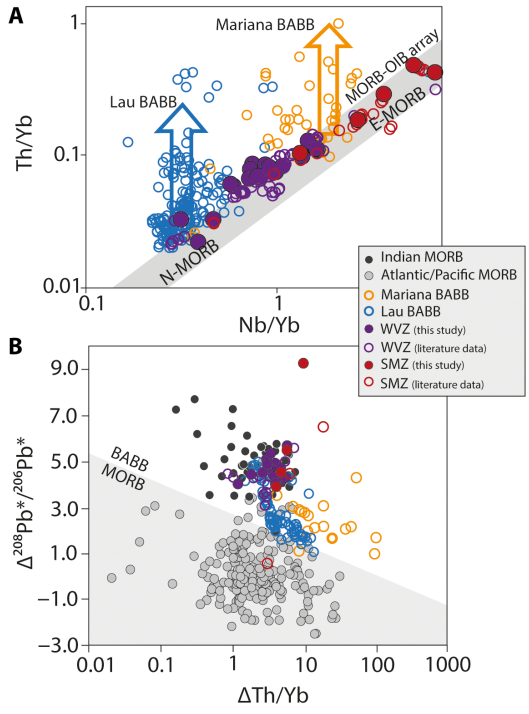

Fig. 6. Th-Nb/Yb covariation diagram and Pb isotope systematics. (**A**) Th-Nb/Yb [after Pearce (*65*)] shows global MORB–ocean island basalt (OIB) array (diagonal gray bar). The orange and dark blue arrows indicate Th/Yb data trends (at a given Nb/Yb) for Lau and Mariana BABB. Many Gakkel Ridge MORBs exceed Th/Yb in the MORB-OIB array at a given Nb/Yb, indicating Th enrichment. MORB data are compiled from Jenner and O'Neill (*64*). (**B**) Elevated mantle Th contents (higher ΔTh/Nb) contribute to high mantle Th/U, producing positive $\Delta^{208}Pb^*/^{206}Pb^*$. ΔTh/Nb is the deviation from the lower boundary of the MORB-OIB array, and $\Delta^{208}Pb^*/^{206}Pb^*$ is the difference in $^{208}Pb/^{206}Pb$ from the NHRL (see the Supplementary Materials for calculation). Mariana and Lau BABB, as well as literature data for the WVZ and the SMZ, are compiled from Gale *et al.* (*63*). Indian, Atlantic, and Pacific MORB data are compiled from Gale *et al.* (*63*). Atlantic MORB data comprise data from 30°N to 30°S and the Pacific MORB data from 12°N to 30°S, respectively.

the (in-)effectiveness of mantle convection to homogenize the upper mantle and how subduction-induced mantle becomes incorporated into ocean floor basalts.

MATERIALS AND METHODS

Seventeen fresh basalts (whole rock) with no visible alteration, including volcanic glasses, from the WVZ and five basalts from the SMZ were analyzed for their major and trace elements, as well as their Sr and Pb isotopes. The chosen sample set is complementary to the preexisting dataset from the Gakkel Ridge (*14*, *26*). Before analysis, volcanic glass samples were ultrasonicated with ultrapure water and ethanol to remove loosely held weathering minerals. Basalt specimens were sawn to remove weathering rinds, washed with ultrapure water in an ultrasonic bath, and crushed in a jaw crusher. Rock chips and volcanic glass fragments were powdered in an agate swing mill. The location of each sample is provided in table S1 and highlighted in Fig. 1.

Major elements

Major element concentrations of the, in total, 22 powdered samples were determined on a PANalytical Axios Advanced WDS x-ray fluorescence (XRF) instrument equipped with a 4000-W Rh x-ray tube at the School of Earth Sciences, University of Tasmania. Each sample (500 mg) was mixed with 12:22 lithium metaborate and lithium tetraborate flux and fused to a glass using a Claisse M4 fluxer. Counting times for each element ranged from 4 to 68 s for a total analysis time of ~8 min per sample. On each individual sample, the loss on ignition (LOI) was determined using ~2 g of the sample powder and heated up to 1000°C for 12 hours. Major element and LOI results are provided in data file S1.

Trace elements

Trace element concentrations of the basalts were determined by laser ablation inductively coupled plasma mass spectrometry (ICP-MS) of 20 basalt (fused discs used for XRF analysis) and two volcanic glass samples. Fragments of both were mounted in 1-inch epoxy discs and analyzed under the same ablation conditions at the Monash Isotopia Laboratory at the School of Earth, Atmosphere and Environment using an ASI RESOlution-SE (S-155) 193-nm ArF excimer laser coupled to Thermo Fisher Scientific icapQ (radio frequency power = 1548 W; ablation cell gas flow = 550 ml min^{-1} He + 0.06 ml min^{-1} N_2; auxiliary gas flow = 1.0 liter min^{-1} Ar). The oxide production (ThO^+/Th^+) at the ICP-MS was kept below <0.7%, and the Th/U ratio was 0.98. Each fused disc and volcanic glass fragment were analyzed for 42 elements (Na, Mg, Al, Si, Ca, Sc, Ti, V, Cr, Mn, Fe, Co, Ni, Zn, Ga, Rb, Sr., Y, Zr, Nb, Mo, Cs, Ba, La, Ce, Pr, Nd, Sm, Eu, Gd, Tb, Dy, Ho, Er, Tm, Yb, Lu, Hf, Ta, Pb, Th, and U) using a spot size of 80 μm, a repetition rate of 10 Hz, and an energy density of 3 J/cm^2; four to five spots were measured on each sample as a transect through the fragment. A single analysis comprised a 20 s gas blank, 30 s data acquisition, and 20 s washout. Blocks of 20 unknowns were bracketed by two to three ablations each of NIST610, NIST612, BCR2G, and BHVO2G. BCR2G was used as calibration standard, while NIST612 (*55*), NIST610 (*55*), and BHVO2G (*56*) were used as quality controls. All results for unknowns and quality controls are reported in data file S1. ^{29}Si (as determined by XRF) was used as internal calibration standard, due to higher contents of SiO_2 of the basalts. For the elements of particular interest here (Ba, Th, Nb, Zr, and Yb), relative standard errors (%RSE) of 0.18%, 0.93%, 1.53%, 2.3%, and 0.11%, respectively, were obtained for a suite of 16 analyses (in total) of the BHVO2G glass. Data were acquired in a time-resolved analysis mode and were reduced using an MS Excel spreadsheet developed at the Max Planck Institute for Chemistry (MPIC) Mainz, Germany (*57*, *58*). An important consideration in chemical analysis of fused discs is the blank of the flux material. The flux material contains 46.74 weight % Si, and Na, Mg, Al, Ca, Ti, and Fe range from 20 parts per million (ppm) (Mg) to 230 ppm (Ca). Apart from Sc, V, and Mn (5, 4, and 8 ppm, respectively), all other measured elements are below 1 ppm (e.g., 0.87-ppm Ba, 0.05-ppm Nb, and 0.33-ppm Zr; Th and Yb are below detection) (data file S1).

Sr and Pb isotope ratios

Pb isotope ratios were acquired from small (1 to 2 mm) chips picked under the microscope. Picked rock chips (150 to 200 mg) were weighed into teflon beakers and leached with hot 6 M HCl (60 min, 100°C). After removal of the leach solution and repeated rinsing with distilled water, residues were dissolved in 5:1 HF-HNO_3 (3 ml, 48 hours, 100°C) on a hot plate. After evaporation of the acid, the residues were refluxed and dried twice with 2 ml of concentrated HNO_3, followed by dissolution with 6 M HCl. Lead was extracted

using a double pass on small beds of AG1-X8 (100 to 200 μm) anion resin. The procedural blank for Pb was 30 ± 10 pg. Lead isotope ratios were measured on a Nu Plasma MC-ICP-MS at the University of Melbourne and on a Thermo Fisher Neptune Plus MC-ICP-MS at the Monash Isotopia Laboratory at the School of Earth, Atmosphere and Environment. Instrumental mass bias was corrected using the thallium-doping technique of Woodhead (*59*). This technique uses separate empirically determined Pb versus Tl isotope correlation lines for each Pb isotope ratio and produces external precisions in the sub-0.1% range (2 SD). For example, U.S. Geological Survey basalt BCR-2 (unleached) measured at the University of Melbourne averages $^{206}Pb/^{204}Pb$ 18.758 ± 0.047%, $^{207}Pb/^{204}Pb$ 15.619 ± 0.066%, and $^{208}Pb/^{204}Pb$ 38.726 ± 0.090% [2 SD, $n = 47$; (*60*)]. A similar approach for the data acquired on the Neptune Plus at the Monash Isotopia Facility yielded averages of 16.941 ± 0.039%, 15.499 ± 0.042%, and 36.722 ± 0.036% (2 SD, $n = 11$) for SRM981. BCR2 averaged 18.750 ± 0.043%, 15.615 ± 0.051%, and 38.691 ± 0.041% (2 SD, $n = 4$). These data are consistent with reference values [(*58*) or http://georem.mpch-mainz.gwdg.de]. Lead isotope data is provided in table S2.

For Sr isotope analyses, ca. 100 mg of sample powder was dissolved as described above and Sr was separated using EICHROM Sr spec (100 to 150 μm) following Pin *et al.* (*61*). The procedural blank was negligible (~60 ± 20 pg). Strontium isotope ratios were measured on a Thermo Fisher Neptune Plus MC-ICP-MS at the Monash Isotopia Laboratory at the School of Earth, Atmosphere and Environment, with sample introduction via a cyclonic glass spray chamber in wet-plasma mode. All measured signal intensities were corrected for memory and Rb-Kr isobars, and instrumental mass bias was corrected by internal normalization to $^{86}Sr/^{88}Sr$ of 0.1194 using the exponential law. Krypton interferences were corrected by using eight iterations of $^{86}Kr/^{84}Kr = 0.30354$ to account for isobaric interferences on ^{86}Sr. $^{87}Sr/^{86}Sr$ in SRM987 averaged 0.710347 ± 0.000062 (2 SD, $n = 15$), and $^{87}Sr/^{86}Sr$ in all runs was adjusted to a more typical value [$^{87}Sr/^{86}Sr = 0.710248$; (*62*)]. Strontium isotope data are provided in table S2.

SUPPLEMENTARY MATERIALS

Supplementary material for this article is available at http://advances.sciencemag.org/cgi/content/full/6/44/eabb4340/DC1

REFERENCES AND NOTES

1. S. R. Hart, A large-scale isotope anomaly in the Southern Hemisphere mantle. *Nature* **309**, 753–757 (1984).
2. C. M. Meyzen, J. Blichert-Toft, J. N. Ludden, E. Humler, C. Mével, F. Albarède, Isotopic portrayal of the Earth's upper mantle flow field. *Nature* **447**, 1069–1074 (2007).
3. J. J. Standish, H. J. B. Dick, P. J. Michael, W. G. Melson, T. O'Hearn, MORB generation beneath the ultraslow spreading Southwest Indian Ridge (9-25°E): Major element chemistry and the importance of process versus source. *Geochem. Geophys. Geosyst.* **9**, Q05004 (2008).
4. J. M. Warren, N. Shimizu, C. Sakaguchi, H. J. B. Dick, E. Nakamura, An assessment of upper mantle heterogeneity based on abyssal peridotite isotopic compositions. *J. Geophys. Res. Solid Earth* **114**, B12203 (2009).
5. V. J. M. Salters, The generation of mid-ocean ridge basalts from the Hf and Nd isotope perspective. *Earth Planet. Sci. Lett.* **141**, 109–123 (1996).
6. A. Stracke, Earth's heterogeneous mantle: A product of convection-driven interaction between crust and mantle. *Chem. Geol.* **330-331**, 274–299 (2012).
7. A. W. Hofmann, Sampling mantle heterogeneity through oceanic basalts: Isotopes and trace elements. *Treatise Geochem.* **2**, 67–101 (2014).
8. M. Rehkämper, A. W. Hofmann, Recycled ocean crust and sediment in Indian Ocean MORB. *Earth Planet. Sci. Lett.* **147**, 93–106 (1997).
9. T. Elliott, A. Thomas, A. Jeffcoate, Y. Niu, Lithium isotope evidence for subduction-enriched mantle in the source of mid-ocean-ridge basalts. *Nature* **443**, 565–568 (2006).
10. M. B. Andersen, T. Elliott, H. Freymuth, K. W. W. Sims, Y. Niu, K. A. Kelley, The terrestrial uranium isotope cycle. *Nature* **517**, 356–359 (2015).
11. S. G. Nielsen, T. J. Horner, H. V. Pryer, J. Blusztajn, Y. Shu, M. D. Kurz, V. le Roux, Barium isotope evidence for pervasive sediment recycling in the upper mantle. *Sci. Adv.* **4**, eaas8675 (2018).
12. S. A. Gibson, M. A. Richards, Delivery of deep-sourced, volatile-rich plume material to the global ridge system. *Earth Planet. Sci. Lett.* **499**, 205–218 (2018).
13. H. J. B. Dick, H. Zhou, Ocean rises are products of variable mantle composition, temperature and focused melting. *Nat. Geosci.* **8**, 68–74 (2014).
14. S. L. Goldstein, G. Soffer, C. H. Langmuir, K. A. Lehnert, D. W. Graham, P. J. Michael, Origin of a 'Southern Hemisphere' geochemical signature in the Arctic upper mantle. *Nature* **453**, 89–93 (2008).
15. C. Z. Liu, J. E. Snow, E. Hellebrand, G. Brügmann, A. von der Handt, A. Büchl, A. W. Hofmann, Ancient, highly heterogeneous mantle beneath Gakkel ridge, Arctic Ocean. *Nature* **452**, 311–316 (2008).
16. M. E. D'Errico, J. M. Warren, M. Godard, Evidence for chemically heterogeneous Arctic mantle beneath the Gakkel Ridge. *Geochim. Cosmochim. Acta* **174**, 291–312 (2016).
17. P. J. Michael, C. H. Langmuir, H. J. B. Dick, J. E. Snow, S. L. Goldstein, D. W. Graham, K. Lehnert, G. Kurras, W. Jokat, R. Mühe, H. N. Edmonds, Magmatic and amagmatic seafloor generation at the ultraslow-spreading Gakkel ridge, Arctic Ocean. *Nature* **423**, 956–961 (2003).
18. M. C. Schmidt-Aursch, W. Jokat, 3D gravity modelling reveals off-axis crustal thickness variations along the western Gakkel Ridge (Arctic Ocean). *Tectonophysics* **691**, 85–97 (2016).
19. J. M. Whittaker, R. D. Muller, W. R. Roest, P. Wessel, W. H. Smith, How supercontinents and superoceans affect seafloor roughness. *Nature* **456**, 938–941 (2008).
20. G. E. Shephard, R. D. Müller, M. Seton, The tectonic evolution of the Arctic since Pangea breakup: Integrating constraints from surface geology and geophysics with mantle structure. *Earth Sci. Rev.* **124**, 148–183 (2013).
21. C. Gaina, S. Medvedev, T. H. Torsvik, I. Koulakov, S. C. Werner, 4D Arctic: A glimpse into the structure and evolution of the Arctic in the light of new geophysical maps, plate tectonics and tomographic models. *Surv. Geophys.* **35**, 1095–1122 (2014).
22. G. E. Shephard, S. Wiers, E. Bazhenova, L. F. Pérez, L. M. Mejía, C. Johansson, M. Jakobsson, M. O'Regan, A North Pole thermal anomaly? Evidence from new and existing heat flow measurements from the central Arctic Ocean. *J. Geodyn.* **118**, 166–181 (2018).
23. G. E. Shephard, R. G. Trønnes, W. Spakman, I. Panet, C. Gaina, Evidence for slab material under Greenland and links to cretaceous high Arctic magmatism. *Geophys. Res. Lett.* **43**, 3717–3726 (2016).
24. A. Stracke, J. E. Snow, E. Hellebrand, A. von der Handt, B. Bourdon, K. Birbaum, D. Günther, Abyssal peridotite Hf isotopes identify extreme mantle depletion. *Earth Planet. Sci. Lett.* **308**, 359–368 (2011).
25. R. Mühe, C. W. Devey, H. Bohrmann, Isotope and trace element geochemistry of MORB from the Nansen-Gakkel ridge at 86° north. *Earth Planet. Sci. Lett.* **120**, 103–109 (1993).
26. A. Gale, C. H. Langmuir, C. A. Dalton, The global systematics of ocean ridge basalts and their origin. *J. Petrol.* **55**, 1051–1082 (2014).
27. F. Nauret, J. E. Snow, E. Hellebrand, D. Weis, Geochemical composition of K-rich lavas from the Lena Trough (Arctic Ocean). *J. Petrol.* **52**, 1185–1206 (2011).
28. S. H. Choi, K. Suzuki, S. B. Mukasa, J.-I. Lee, H. Jung, Lu–Hf and Re–Os systematics of peridotite xenoliths from Spitsbergen, western Svalbard: Implications for mantle–crust coupling. *Earth Planet. Sci. Lett.* **297**, 121–132 (2010).
29. J. C. Lassiter, B. L. Byerly, J. E. Snow, E. Hellebrand, Constraints from Os-isotope variations on the origin of Lena Trough abyssal peridotites and implications for the composition and evolution of the depleted upper mantle. *Earth Planet. Sci. Lett.* **403**, 178–187 (2014).
30. F. Nauret, M. Moreira, J. E. Snow, Rare gases in lavas from the ultraslow spreading Lena Trough, Arctic Ocean. *Geochem. Geophys. Geosyst.* **11**, (2010).
31. J. C. Lassiter, E. H. Hauri, Osmium-isotope variations in Hawaiian lavas: Evidence for recycled oceanic lithosphere in the Hawaiian plume. *Earth Planet. Sci. Lett.* **164**, 483–496 (1998).
32. K. C. Condie, in *Earth as an Evolving Planetary System*, K. C. Condie, Ed. (Academic Press, ed. 3, 2016), pp. 147–199.
33. J. A. Pearce, R. J. Stern, in *Back-Arc Spreading Systems: Geological, Biological, Chemical, and Physical Interactions* (American Geophysical Union, 2013), pp. 63–86.
34. R. Kessel, M. W. Schmidt, P. Ulmer, T. Pettke, Trace element signature of subduction-zone fluids, melts and supercritical liquids at 120–180 km depth. *Nature* **437**, 724–727 (2005).
35. J. A. Pearce, R. J. Stern, S. H. Bloomer, P. Fryer, Geochemical mapping of the Mariana arc-basin system: Implications for the nature and distribution of subduction components. *Geochem. Geophys. Geosyst.* **6**, (2005).
36. C. Spandler, C. Pirard, Element recycling from subducting slabs to arc crust: A review. *Lithos* **170-171**, 208–223 (2013).
37. D. G. van der Meer, D. J. J. van Hinsbergen, W. Spakman, Atlas of the underworld: Slab remnants in the mantle, their sinking history, and a new outlook on lower mantle viscosity. *Tectonophysics* **723**, 309–448 (2018).
38. S. G. Nielsen, H. R. Marschall, Geochemical evidence for mélange melting in global arcs. *Sci. Adv.* **3**, e1602402 (2017).

39. Y. Shu, S. G. Nielsen, H. R. Marschall, T. John, J. Blusztajn, M. Auro, Closing the loop: Subducted eclogites match thallium isotope compositions of ocean island basalts. *Geochim. Cosmochim. Acta* **250**, 130–148 (2019).
40. H. R. Marschall, J. C. Schumacher, Arc magmas sourced from mélange diapirs in subduction zones. *Nat. Geosci.* **5**, 862–867 (2012).
41. C. J. Hawkesworth, S. P. Turner, F. Mc Dermott, D. W. Peate, P. van Calsteren, U-Th isotopes in arc magmas: Implications for element transfer from the subducted crust. *Science* **276**, 551–555 (1997).
42. W. M. White, 238U/204Pb in MORB and open system evolution of the depleted mantle. *Earth Planet. Sci. Lett.* **115**, 211–226 (1993).
43. H. S. O'Neill, F. E. Jenner, The global pattern of trace-element distributions in ocean floor basalts. *Nature* **491**, 698–704 (2012).
44. B. Wunder, S. Melzer, Experimental evidence on phlogopitic mantle metasomatism induced by phengite dehydration. *Eur. J. Mineral.* **15**, 641–647 (2003).
45. E. J. Catlos, S. S. Sorensen, Phengite-based chronology of K- and Ba-rich fluid flow in two paleosubduction zones. *Science* **299**, 92–95 (2003).
46. S. S. Sorensen, J. N. Grossman, M. R. Perfit, Phengite-hosted LILE enrichment in eclogite and related rocks: Implications for fluid-mediated mass transfer in subduction zones and arc magma genesis. *J. Petrol.* **38**, 3–34 (1997).
47. S. Lebedev, A. J. Schaeffer, J. Fullea, V. Pease, Seismic tomography of the Arctic region: Inferences for the thermal structure and evolution of the lithosphere. *Geol. Soc. Lond. Spec. Publ.* **460**, 419–440 (2018).
48. A. J. Schaeffer, S. Lebedev, Global shear speed structure of the upper mantle and transition zone. *Geophys. J. Int.* **194**, 417–449 (2013).
49. G. E. Shephard, N. Flament, S. Williams, M. Seton, M. Gurnis, R. D. Müller, Circum-Arctic mantle structure and long-wavelength topography since the Jurassic. *J. Geophys. Res. Solid Earth* **119**, 7889–7908 (2014).
50. A. Alvey, C. Gaina, N. J. Kusznir, T. H. Torsvik, Integrated crustal thickness mapping and plate reconstructions for the high Arctic. *Earth Planet. Sci. Lett.* **274**, 310–321 (2008).
51. P. D. Kempton, J. A. Pearce, T. L. Barry, J. G. Fitton, C. Langmuir, D. M. Christie, Sr-Nd-Pb-Hf isotope results from ODP Leg 187: Evidence for mantle dynamics of the Australian-Antarctic discordance and origin of the Indian MORB source. *Geochem. Geophys. Geosyst.* **3**, 1–35 (2002).
52. M. Gurnis, R. D. Müller, in *Evolution and Dynamics of the Australian Plate*, R. R. Hillis, R. D. Müller, Eds. (Geological Society of America, 2003).
53. O. Nebel, C. Münker, Y. J. Nebel-Jacobsen, T. Kleine, K. Mezger, N. Mortimer, Hf–Nd–Pb isotope evidence from Permian arc rocks for the long-term presence of the Indian–Pacific mantle boundary in the SW Pacific. *Earth Planet. Sci. Lett.* **254**, 377–392 (2007).
54. P. A. Cawood, Terra Australis Orogen: Rodinia breakup and development of the Pacific and Iapetus margins of Gondwana during the Neoproterozoic and Paleozoic. *Earth Sci. Rev.* **69**, 249–279 (2005).
55. K. P. Jochum, U. Weis, B. Stoll, D. Kuzmin, Q. Yang, I. Raczek, D. E. Jacob, A. Stracke, K. Birbaum, D. A. Frick, D. Günther, J. Enzweiler, Determination of reference values for NIST SRM 610–617 glasses following ISO guidelines. *Geostand. Geoanal. Res.* **35**, 397–429 (2011).
56. K. P. Jochum, M. Willbold, I. Raczek, B. Stoll, K. Herwig, Chemical characterisation of the USGS reference glasses GSA-1G, GSC-1G, GSD-1G, GSE-1G, BCR-2G, BHVO-2G and BIR-1G Using EPMA, ID-TIMS, ID-ICP-MS and LA-ICP-MS. *Geostand. Geoanal. Res.* **29**, 285–302 (2005).
57. H. P. Longerich, S. E. Jackson, D. Gunther, Inter-laboratory note. Laser ablation inductively coupled plasma mass spectrometric transient signal data acquisition and analyte concentration calculation. *J. Anal. At. Spectrom.* **11**, 899–904 (1996).
58. K. P. Jochum, B. Stoll, K. Herwig, M. Willbold, Validation of LA-ICP-MS trace element analysis of geological glasses using a new solid-state 193 nm Nd:YAG laser and matrix-matched calibration. *J. Anal. At. Spectrom.* **22**, 112–121 (2007).
59. J. Woodhead, A simple method for obtaining highly accurate Pb isotope data by MC-ICP-MS. *J. Anal. At. Spectrom.* **17**, 1381–1385 (2002).
60. R. Maas, E. S. Grew, C. J. Carson, Isotopic constraints (Pb, Rb-Sr, Sm-Nd) on the sources of Early Cambrian Pegmatites with Boron and Beryllium minerals in the Larsemann Hills, Prydz Bay, Antarctica. *Can. Mineral.* **53**, 249–272 (2015).
61. C. Pin, D. Briot, C. Bassin, F. Poitrasson, Concomitant separation of strontium and samarium-neodymium for isotopic analysis in silicate samples, based on specific extraction chromatography. *Anal. Chim. Acta* **298**, 209–217 (1994).
62. J. M. McArthur, Recent trends in strontium isotope stratigraphy. *Terra Nova* **6**, 331–358 (1994).
63. A. Gale, C. A. Dalton, C. H. Langmuir, Y. Su, J.-G. Schilling, The mean composition of ocean ridge basalts. *Geochem. Geophys. Geosyst.* **14**, 489–518 (2013).
64. F. E. Jenner, H. S. C. O'Neill, Analysis of 60 elements in 616 ocean floor basaltic glasses. *Geochem. Geophys. Geosyst.* **13**, Q02005 (2012).
65. J. A. Pearce, Geochemical fingerprinting of oceanic basalts with applications to ophiolite classification and the search for Archean oceanic crust. *Lithos* **100**, 14–48 (2008).
66. C. J. Allègre, B. Dupré, E. Lewin, Thorium/uranium ratio of the Earth. *Chem. Geol.* **56**, 219–227 (1986).
67. M. Tatsumoto, Isotopic composition of lead in oceanic basalt and its implication to mantle evolution. *Earth Planet. Sci. Lett.* **38**, 63–87 (1978).
68. R. D. Müller, M. Seton, S. Zahirovic, S. E. Williams, K. J. Matthews, N. M. Wright, G. E. Shephard, K. T. Maloney, N. Barnett-Moore, M. Hosseinpour, D. J. Bower, J. Cannon, Ocean basin evolution and global-scale plate reorganization events since Pangea breakup. *Annu. Rev. Earth Planet. Sci.* **44**, 107–138 (2016).
69. R. D. Müller, J. Cannon, X. Qin, R. J. Watson, M. Gurnis, S. Williams, T. Pfaffelmoser, M. Seton, S. H. J. Russell, S. Zahirovic, GPlates: Building a virtual Earth through deep time. *Geochem. Geophys. Geosyst.* **19**, 2243–2261 (2018).
70. C. J. Grose, Properties of oceanic lithosphere: Revised plate cooling model predictions. *Earth Planet. Sci. Lett.* **333-334**, 250–264 (2012).
71. B. Parsons, J. G. Sclater, An analysis of the variation of ocean floor bathymetry and heat flow with age. *J. Geophys. Res.* **82**, 803–827 (1977).
72. C. A. Stein, S. Stein, A model for the global variation in oceanic depth and heat flow with lithospheric age. *Nature* **359**, 123–129 (1992).

Acknowledgments: We would like to acknowledge J. Thompson from UTAS (now at the NASA Johnson Space Center) for undertaking the major element analysis at the XRF facility CODES and Massimo Raveggi from the Isotopia Laboratory for his help with LA-ICP-MS analysis. We would also like to thank Wolfgang Bach (University of Bremen) for providing additional samples for this study. We thank M. Finch and A. Tomkins for discussions. Furthermore, we thank S. Goldstein and M. Roden for comments on an early version of this manuscript. We would like to thank two anonymous reviewers for their constructive feedback. Last but not least, we thank C.-T. Lee for the editorial handling of this manuscript. **Funding:** O.N. was supported by the Australian Research Council (grant FT140101062). P.A.C. was supported by the Australian Research Council (grant FL160100168). H.J.B.D. was supported by the NSF (grants PLR 9912162, PLR 0327591, OCE 0930487, and OCE 1434452). M.R. was supported by a graduate scholarship of Monash University and the SEAE. **Author contributions:** M.R. acquired samples and data and wrote the first draft of the manuscript. M.R. and O.N. designed the study, discussed the data, and wrote the final version of the manuscript. R.M. performed the purification of Pb in the clean laboratory. B.M. assisted with the plate reconstructions and geodynamic modeling. R.M. and Y.N.-J. assisted with the isotope analyses. P.A.C. provided guidance of research and revised early versions of this manuscript. H.J.B.D. provided the samples. F.A.C. helped with the discussion of geodynamic principles. All authors contributed to the editing of the manuscript. **Competing interests:** The authors declare that they have no competing interests. **Data and materials availability:** All data needed to evaluate the conclusions in the paper are present in the paper and/or the Supplementary Materials. Additional data related to this paper may be requested from the authors.

Submitted 25 February 2020
Accepted 14 September 2020
Published 30 October 2020
10.1126/sciadv.abb4340

Citation: M. Richter, O. Nebel, R. Maas, B. Mather, Y. Nebel-Jacobsen, F. A. Capitanio, H. J. B. Dick, P. A. Cawood, An Early Cretaceous subduction-modified mantle underneath the ultraslow spreading Gakkel Ridge, Arctic Ocean. *Sci. Adv.* **6**, eabb4340 (2020).

Science Advances

An Early Cretaceous subduction-modified mantle underneath the ultraslow spreading Gakkel Ridge, Arctic Ocean

Marianne Richter, Oliver Nebel, Roland Maas, Ben Mather, Yona Nebel-Jacobsen, Fabio A. Capitanio, Henry J. B. Dick and Peter A. Cawood

Sci Adv **6** (44), eabb4340.
DOI: 10.1126/sciadv.abb4340